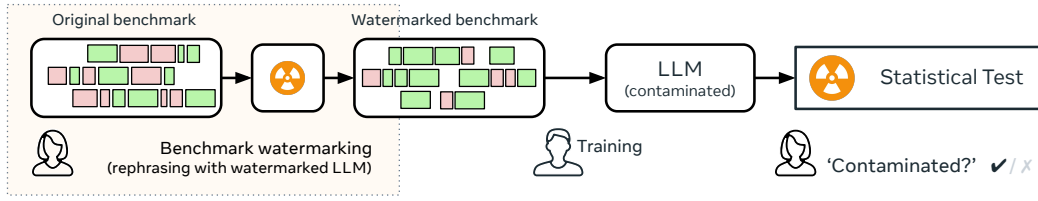


000 001 002 003 004 005 DETECTING BENCHMARK CONTAMINATION 006 THROUGH WATERMARKING 007 008

009 **Anonymous authors**
010 Paper under double-blind review
011
012
013
014
015
016
017
018
019
020

021 ABSTRACT 022

023 Benchmark contamination undermines LLM evaluations, and existing post-hoc
024 detection methods are [heuristics](#) and thus lack verifiable guarantees. We propose a
025 proactive solution: embedding cryptographic watermarks into benchmarks *before*
026 their release through question reformulation with a language model, and introduce a
027 detection algorithm that overcomes tokenizer mismatches by aligning text prefixes
028 to reliably identify the watermark signal in the suspect model. To validate our
029 method, we pre-train 1B-parameter models on 10B tokens with controlled con-
030 tamination of MMLU and ARC. The watermarking process preserves benchmark
031 utility, while our test detects contamination with high confidence, achieving, *e.g.*, a
032 p -value $< 10^{-5}$ for a mere 5% performance gain on 5000 MMLU questions.
033



034 Figure 1: Problem overview. *Alice* is a benchmark provider. Before release, she rephrases the original benchmark
035 dataset while embedding a watermark. *Bob* decides to train a model. The benchmark may contaminate Bob’s
036 model during training. Alice can give statistical evidence if her benchmark was used in training.
037

038 1 INTRODUCTION 039

040 In recent years, Large Language Models (LLMs) have demonstrated remarkable advancements in
041 their capabilities (Brown et al., 2020; Touvron et al., 2023a). This advancement places increasingly
042 greater emphasis on proper evaluation to both inform the state of LLM research and to guide
043 future developments. To this end, a multitude of benchmark datasets such as (MMLU) (Hendrycks
044 et al., 2020), School Math 8K (GSM8K) (Cobbe et al., 2021), and the AI2 Reasoning Challenge
045 (ARC) (Clark et al., 2018), or more recently GPQA (Rein et al., 2023) and FrontierMath (Glazer et al.,
046 2024), are developed to measure the model’s capabilities in terms of general or specific knowledge,
047 understanding, and scientific reasoning.
048

049 The reliability of LLM evaluation is critically undermined by benchmark contamination. While
050 drops in performance on rephrased benchmarks such as the recent GSM8K variant (Zhang et al.,
051 2024a) strongly suggest contamination, they do not provide definitive proof, leaving the community
052 to debate the validity of a model’s claimed capabilities. This uncertainty stems from the fundamental
053 limitations of existing post-hoc detection methods. These methods analyze a model after training and
054 are ultimately [heuristics](#), *i.e.*, they rely on indirect evidence and observable patterns rather than direct
055 proof of contamination. For instance, methods like Membership Inference Attacks (MIAs) rely on a
056 held-out set from the same data distribution. This requirement is a paradox for public benchmarks: if
057 such a set existed, it could simply serve as the new, uncontaminated benchmark. This gap reveals
058 the need for a shift from post-hoc suspicion to proactive, verifiable proof. Instead of trying to find
059 evidence of contamination after the fact, we argue that the community must embed a provable but
060 undetectable signal into benchmarks before their release. Our work introduces such a framework.
061

We propose a novel strategy of embedding non-intrusive watermarks in the benchmark dataset before release. Our approach is inspired by Sander et al. (2024), who demonstrated that slightly distilling a watermarked LLM can be reliably detected, as the model retains identifiable traces of the watermark. We extend this idea to dataset watermarking, and when possibly different tokenizers are used by the watermarking and the suspect models. Our approach enables reporting both model performance on the benchmark and a reliable p -value as a contamination score, which relates to the False Positive Rate of the contamination test (see Proposition 1). If the reported p -value is low, the LLM’s training data is likely contaminated with the benchmark dataset and the performance numbers should not be trusted as genuine. Our method requires only access to an LLM capable of rephrasing benchmark questions; see Figure 1 for an overview, and operates in a white-box setting to detect contamination, which would work for open source models and self auditing for closed ones. Our contributions are:

- **A proactive framework for detecting pre-training contamination.** We adapt the concept of watermark radioactivity (Sander et al., 2024), previously applied to instruction-tuning data, to the distinct and more challenging problem of detecting pre-training data contamination. Our method proactively embeds a secret statistical signal into benchmarks via a rephrasing LLM prior to their release – while safeguarding utility – in order to later provide provable evidence of contamination.
- **A robust, cross-tokenizer detection algorithm.** Recognizing the diversity of tokenizers in the LLM ecosystem, we introduce a novel detection algorithm that reliably identifies the watermark signal even when a suspect model uses a different tokenizer from the one used for embedding. This contribution significantly enhances the practical applicability of our method for auditing a wide range of models (Algorithm 1 in Sec. 3.2).
- **Extensive empirical validation and comparison.** We provide a large-scale empirical validation of this proactive detection method by pre-training models of up to 1B parameters on 10B tokens. Our experiments demonstrate strong correlation between the detection confidence and the performance inflation caused by contamination. They also show that our method is significantly more sensitive than comparable baselines like canaries. For instance, we detect contamination with a p -value below 10^{-5} when accuracy is inflated by only 5% on MMLU, while correctly yielding p -values near 0.5 for uncontaminated models (Figure 3b and Table 1).

Our code will be made available to enable post-hoc text watermarking and contamination detection.

2 RELATED WORK

2.1 BENCHMARK CONTAMINATION DETECTION

Benchmark contamination is a significant concern that can lead to unreliable LLM evaluations (Singh et al., 2024; Balloccu et al., 2024). The issue is pervasive, as even rigorous decontamination efforts are not foolproof (Brown et al., 2020; Singh et al., 2024), and small amounts of contamination can significantly inflate performance (Jiang et al., 2024). The existence of this problem has been convincingly demonstrated by studies like the one by Zhang et al. (2024a). They crafted new questions for GSM8K and observed a significant drop in performance for most models, suggesting memorization of the original test set.

While a variety of post-hoc methods exist to detect contamination – from membership inference attacks (MIAs) (Carlini et al., 2022) to analyzing performance on reformulated questions (Yang et al., 2023; Duarte et al., 2024) or on reordered answers (Oren et al., 2023) – they are fundamentally **heuristics** and face practical limitations. For instance, many require a held-out set, which is a paradoxical requirement for public benchmarks. Recent work has also shown that MIAs suffer from distribution shifts, further complicating efforts to reliably detect contamination (Meeus et al., 2025).

For active methods, the work most similar to ours is the contemporary paper by Rastogi et al. (2025), which approaches dataset membership inference by generating multiple rephrased versions of a benchmark. Each version is embedded with a unique watermark, yet only one is released publicly. By employing a paired t-test to compare the model’s perplexity on the public version against the withheld private versions, their method identifies training inclusion based on the model’s statistical preference for the specific public watermark. However, similar to other MIAs such as Maini et al. (2024), contamination detection for STAMP is restricted to the entity holding the private benchmark versions. Moreover, because it necessitates open-weight (or at least grey-box) access to the model, it

108 thus makes it impractical for evaluating proprietary models. In contrast, our method relies solely on
 109 the official version, enabling any party to perform the contamination test. Our approach is also close
 110 to hiding canaries inside the benchmarks as done in Srivastava et al. (2022), to which we compare
 111 directly as it does not necessitate any held-out.

112 We provide a detailed comparison and discussion of the trade-offs between all methods in 4.3.
 113

114 2.2 DECODING-BASED WATERMARKING & RADIOACTIVITY 115

116 **Overview.** Recent watermarking techniques for large language models (LLMs) involve altering
 117 either the probability distribution (Kirchenbauer et al., 2023a) or the method used for sampling
 118 the subsequent token (Aaronson & Kirchner, 2023; Kuditipudi et al., 2023). Detection of these
 119 watermarks is influenced by the entropy of the generated text (Christ et al., 2023; Huang et al.,
 120 2023), so further investigations propose watermarking only sections with high entropy, especially in
 121 code (Lee et al., 2023), while other studies explore “semantic” watermarks that rely on the semantic
 122 representation of the entire preceding text (Liu et al., 2023; Liu & Bu, 2024; Fu et al., 2024).

123 **Greenlist/redlist watermark.** Our work focuses on the watermarking scheme proposed by Kirchen-
 124 bauer et al. (2023b), which modifies the logit vector during token generation based on a context
 125 window of k previous tokens and a private key s . Both are hashed to serve as the seed for a random
 126 number generator (RNG) to create a “greenlist” of $\gamma|\mathcal{V}|$ tokens, where \mathcal{V} is the vocabulary of the
 127 tokenizer, and $\gamma \in [0, 1]$. Logits of green tokens are incremented by δ to increase their sampling prob-
 128 ability. Detection involves repeating the greenlist computation for each token of a text, incrementing
 129 a score by 1 if the token is in the greenlist, and performing a statistical test on the cumulative score.
 130 Under the null hypothesis \mathcal{H}_0 “the text is not watermarked with that scheme”, this score follows a
 131 binomial distribution (Fernandez et al., 2023). A simple binomial test thus provides a p -value.
 132

133 **Radioactivity of LLM watermarks.** Sander et al. (2024) show that fine-tuning language models
 134 on LLM-generated watermarked question-answer pairs can be detected with high confidence, as
 135 the model retains traces of the watermark bias. The authors adapt the original watermark detection
 136 tests to detect watermark “radioactivity” – a term first coined in Sablayrolles et al. (2020) for image
 137 data – depending on the access to the suspect model and its training data. Similar observations had
 138 been made in other scenarios. For instance, Gu et al. (2023) demonstrate that LLM watermarks
 139 can be intentionally distilled, and [Gloaguen et al. \(2025\) examines model watermarks durability](#)
 140 [post-training](#). Zhao et al. (2023) introduce a signal in generated text that can be learned by other
 141 LLMs trained on it, and Jovanović et al. (2024) investigate watermark radioactivity for RAG. detect
 142 traces inserted during training, but the use case is largely different. Other work deal with embedding
 143 traces in models to detect it a [Elhassan et al. \(2025\) embeds a LoRA-based watermark into weights](#)
 144 [during fine-tuning, aiming to identify the model generator](#).
 145

146 3 METHOD

147 **Scope: threat model and access requirements.** Our work focuses on detecting contamination
 148 in LLMs that do next token-prediction with transformer-based models. Our method principally
 149 targets unintentional benchmark contamination, the common result of indiscriminate web scraping.
 150 Dedicated adversarial attacks, such as paraphrasing to evade detection, are not considered in this work.
 151 Moreover, our detection test operates in a white-box setting, requiring logit access of the suspect
 152 model. This enables transparent auditing of open-source models and supports verifiable self-reporting
 153 of contamination p -values for closed-source developers, fostering greater trust in evaluations.
 154

155 We first focus in Section 3.1 on the task of rephrasing the questions of a benchmark dataset while
 156 embedding a watermark using Kirchenbauer et al. (2023b). Then, in Section 3.2, we show how to
 157 detect if a language model was trained on the watermarked benchmark.

158 3.1 INSERTING WATERMARK THROUGH QUESTION REPHRASING 159

160 We use an instruct language model, denoted as LM_{rephrase} , which is assumed to be capable of
 161 rephrasing each question in the benchmark test set such that the rephrased version is logically
 162 equivalent to the original. This is a pretty light assumption as the task of rephrasing is considerably

162 easier than answering the question (Deng et al., 2023). LM_{rephrase} generates token per token and
 163 at each step, takes as input a context, which is the concatenation of the system prompt, rephrasing
 164 instruction, the question to rephrase and the reformulation generated so far. Everything is tokenized
 165 into a sequence $(x^{(1)}, \dots, x^{(t-1)}) \in \mathcal{V}^{t-1}$, where \mathcal{V} is the vocabulary of the tokenizer.
 166

167 LM_{rephrase} outputs a logits vector $\ell^{(t)} \in \mathbb{R}^{|\mathcal{V}|}$. The watermark embedding modifies $\ell^{(t)}$ based on a
 168 secret key s (one per benchmark) and the watermark window $(x^{(t-k)}, \dots, x^{(t-1)}) \in \mathcal{V}^k$

169 Specifically, following the method of Kirchenbauer et al. (2023b) detailed in Sec. 2.2, a secret-key
 170 cryptographic function hashes s as well as the the watermark window, which serves as a seed for a
 171 random number generator used to create a pseudo-random “greenlist” of tokens, comprising $\gamma = 50\%$
 172 of the entire vocabulary \mathcal{V} , for which the logits are incremented by a quantity δ to form $\tilde{\ell}^{(t)}$, thereby
 173 increasing their probability of being sampled. The logits vector is then transformed into a probability
 174 distribution $\mathbf{p}^{(t)} = \text{softmax}(\tilde{\ell}^{(t)}) \in [0, 1]^{|\mathcal{V}|}$, and the generation proceeds by sampling the next token
 175 $x^{(t)}$ from this distribution using a sampling procedure such as top-k sampling (Fan et al., 2018) or
 176 nucleus sampling (Holtzman et al., 2019). The selected token is appended to the context, and the
 177 process repeats. An example for the watermark embedding process is depicted in Figure 2a, with a
 178 detailed version with different strength of watermarking in Figure 5 of Appendix A.
 179

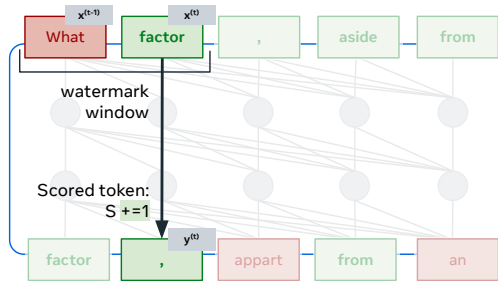
180 **Detectability/utility tradeoff.** There is a common tradeoff in watermarking between detection and
 181 utility. In our case *detection* is the ability to have statistical evidence that the benchmark was used
 182 during training. We show in subsection 3.2 that it can be measured through the p -value, which can
 183 directly be linked to the False Positive Rate of the detection test (see Prop. 1). A lower p -value thus
 184 indicates a stronger detection signal, making it more likely to identify unauthorized usage. On the
 185 other hand, the *utility* of the watermarked benchmark is its ability to rank models and assess their
 186 performance on specific tasks. To preserve utility, we therefore require that models perform similarly
 187 on both the original and watermarked versions of the benchmark, allowing for accurate evaluation
 188 and comparison of model performance. Specifically, the benchmark dataset exhibits a proportion
 189 $\rho > 0.5$ of green tokens after rephrasing, the greater the easier detectability. For utility, we check if
 190 pre-trained models perform similarly on the original and rephrased versions.

191 We envision a practical workflow where benchmark creators are the final arbiters of quality. They
 192 can tune the watermark strength (δ) and rephrasing model, and use a human-in-the-loop process to
 193 validate or select from multiple rephrased candidates, ensuring the benchmark’s integrity.

194 3.2 DETECTING RADIOACTIVITY WITH A STATISTICAL TEST

196 To test a suspect model for contamination, we check for “radioactivity” by analyzing its predictions
 197 on the watermarked benchmark questions in a “reading mode” approach (Sander et al., 2024). That
 198 is, for each question, we forward the N tokens that form the question and observe the N predicted
 199 next tokens. The core idea is that a model contaminated with the benchmark data will have learned
 200 the statistical biases introduced by our watermark, causing its predictions to be skewed towards the
 201 watermark’s “green list”, as illustrated in Fig. 2b.

203 **System prompt + instruction:**
 204 “You are a problem rephrasing assistant [...]”
 205 **Question:** “The rate of acceleration of an object
 206 is determined by the mass of the object and”
 207 **Rephrased with watermark ($\delta = 4$):**
 208 “What factor, aside from an object’s mass, deter-
 209 mines its acceleration?” (73% of green tokens)



212 (a) Embedding - benchmark rephrasing

213 (b) Detection - statistical test

214 Figure 2: Method description. (Left) Watermarking benchmarks’ questions using LLMs, as in subsection 3.1,
 215 with an example from ARC-easy. The quality of the question is maintained. (Right) Reading mode, as detailed
 216 in subsection 3.2. The upper sequence is the watermarked question, and the tokens below are top-1 predictions
 217 from the suspect model.

This allows us to formulate a powerful statistical test based on a clear null hypothesis, \mathcal{H}_0 : an uncontaminated model’s predictions are statistically independent of our secret watermark key, s . Since our scheme partitions the vocabulary into equally sized “green” and “red” lists for any context, a model under \mathcal{H}_0 should predict a green-list token with 50% probability. We can therefore count the number of green-list predictions, S , over a set of \tilde{N} trials. To ensure each trial is independent and identically distributed (i.i.d.), we only score each unique context window once (Fernandez et al., 2023). This count follows a binomial distribution, $S \sim B(\tilde{N}, 1/2)$, and a significantly high score allows us to reject \mathcal{H}_0 and conclude the model is radioactive. The corresponding p -value is calculated using the regularized incomplete Beta function: $p\text{-value}(s) = I_{0.5}(s, \tilde{N} - s + 1)$.

A key practical challenge arises when the suspect model uses a different tokenizer (T_2) from the one used for watermarking (T_1), preventing direct comparison. Our method addresses this with an alignment procedure detailed in Algorithm 1. We tokenize the input with both T_1 and T_2 and only consider a prediction for scoring at “alignment points” where the text prefixes generated by both tokenizers are identical. At these points, we can safely regenerate the green list using the T_1 context. If the predicted token from T_2 also exists in T_1 ’s vocabulary, we score it (incrementing S by 1 if it is green). This ensures our statistical test’s validity across different tokenizers.

Proposition 1. *If we define “being contaminated” as having memorized the watermark (i.e., being radioactive), then the test T_α (that rejects \mathcal{H}_0 if the p -value is less than α) correctly tests for contamination with a False Positive Rate (FPR) equal to α .*

This proposition (proven in Appendix B) confirms that our p -value provides a theoretically grounded measure of contamination. While being radioactive is distinct from having an artificially inflated benchmark score, our results in Section 4 empirically demonstrate a strong correlation.

Algorithm 1: Reading Mode Scoring with Different Tokenizers

Input: Question q from watermarked benchmark, Tokenizer T_1 for watermarking, Tokenizer T_2 of suspect model M , tape \mathcal{T} of already-scored watermark window, score S

Tokenize s with T_1 : x_0, x_1, \dots, x_{n-1} ;

Tokenize s with T_2 : y_0, y_1, \dots, y_{m-1} ;

Get top-1 predictions $\tilde{y}_1, \tilde{y}_2, \dots, \tilde{y}_m$ from M ;

for $i \leftarrow 0$ **to** $m - 1$ **do**

if there exists j where $\text{text}(y_0, \dots, y_i) = \text{text}(x_0, \dots, x_j)$ **then**

if $\tilde{y}_{i+1} \in T_1.\text{vocab}$ **and** $(x_{j-k+1}, \dots, x_j) \notin \mathcal{T}$ **then**

$S += \text{Score}((x_{j-k+1}, \dots, x_j, \tilde{y}_{i+1}))$;

$\mathcal{T}.\text{add}((x_{j-k+1}, \dots, x_j))$;

4 RESULTS

4.1 BENCHMARK QUALITY AFTER WATERMARKING

Set-up. For the watermark embedding, we rephrase with Llama-3.1-8B-Instruct (Dubey et al., 2024) by default, with top-p sampling with $p = 0.7$ and temperature = 0.5 (default values on the Hugging Face hub), and the green/red watermarking scheme of Kirchenbauer et al. (2023b) with a watermark window $k = 2$ and a “greenlist” of size $\frac{1}{2}|\mathcal{V}|$ ($|\mathcal{V}|$ is the vocabulary size). We compare different values of δ when rephrasing: 0 (no watermarking), 1, 2, and 4. We choose to watermark ARC-Challenge, ARC-Easy, and MMLU due to their widespread use in model evaluation. In practice, one would need to watermark their own benchmark before release. For MMLU, we select a subset of 5000 questions, randomly chosen across all disciplines, to accelerate experimentation and maintain a comparable size to the other benchmarks. We refer to this subset as MMLU*. ARC-Easy contains 1172 questions, and ARC-Challenge contains 2372 questions. In Figure 5, we show the exact instructions given to the rephrasing model (identical for all benchmarks) and the results for different watermarking strengths. We use a different watermarking key s for each benchmark.

Even strong watermarking retains benchmark utility. We evaluate the performance of Llama-3.3-1B, Llama-3.3-3B and Llama-3.1-8B on the original benchmark and the rephrased version using

as similar evaluation as the one from the lm-evaluation-harness library (Gao et al., 2024). To check if the benchmark is still as meaningful, we check that evaluated models obtain a similar accuracy on the watermarked benchmarks and on the original version (see subsection 3.1). Figure 3a shows the performance on ARC-Easy. All models perform very similarly on all the rephrased versions of the benchmark, even when pushing the watermark to 80% of green tokens. Importantly, they rank the same. Similar results are shown for MMLU* and ARC-Challenge in Figure 7 of Appendix A, although for MMLU*, we observe some discrepancies. For instance, when using a watermarking window size of 2 (subfig i), the performance of Llama-3.2-1B increases from 38% to 42% between the original and the other versions. However, we observe the same issue when rephrasing without watermarking in that case. As detailed in subsection 3.1, tuning the instruction specifically for each benchmark could help. Note that the choice of δ depends on the benchmark and the rephrasing model, and needs to be empirically tested. [Performance of other models are given in app. D.](#)

4.2 CONTAMINATION DETECTION THROUGH RADIOACTIVITY

We now propose an experimental design to control benchmark contamination, and evaluate both the impact on model performance and on contamination detection.

Training set-up. We train 1B [standard decoder-only transformer architecture with the causal language modeling objective similar to the foundational T-decoder](#) (Liu et al., 2018) and GPT (Radford & Narasimhan, 2018), adapted from the encoder-decoder architecture proposed in Vaswani et al. (2017) using Meta Lingua (Videau et al., 2024) and the code-base’s default architectural choices. We train on 10B tokens from DCLM (Li et al., 2024), with the same tokenizer used to embed the watermark, unless stated otherwise (e.g., in Sec. 4.5). The model architecture includes a hidden dimension of 2048, 25 layers, and 16 attention heads. The training process consists of 10,000 steps, using a batch size of 4 and a sequence length of 4096. Each training is distributed across 64 A-100 GPUs, and takes approximately three hours to finish. The optimization is performed with a learning rate of 3×10^{-3} , a weight decay of 0.033, and a warmup period of 5,000 steps. The learning rate is decayed to a minimum ratio of 10^{-6} , and gradient clipping is applied with a threshold of 1.0.

Contamination set-up. Between training steps 2,500 and 7,500, we perform contamination by replacing a training batch from the DCLM corpus with a batch sampled from the shuffled concatenation of the three watermarked benchmarks. This batch replacement occurs periodically, specifically every 5000 / #ContaminationSteps training steps. Each batch has batch size \times sequence length \times number of GPUs = $4 \times 4096 \times 64 \approx 1$ M tokens. As shown in Table 1, the concatenation of the three benchmarks is approximately 500k tokens, so each contamination is a gradient that encompasses all the benchmark’s tokens. Any sample that contaminates the model is formatted as: f"Question: {Question}\nAnswer: {Answer}" In the experiments, #ContaminationSteps is referred as the

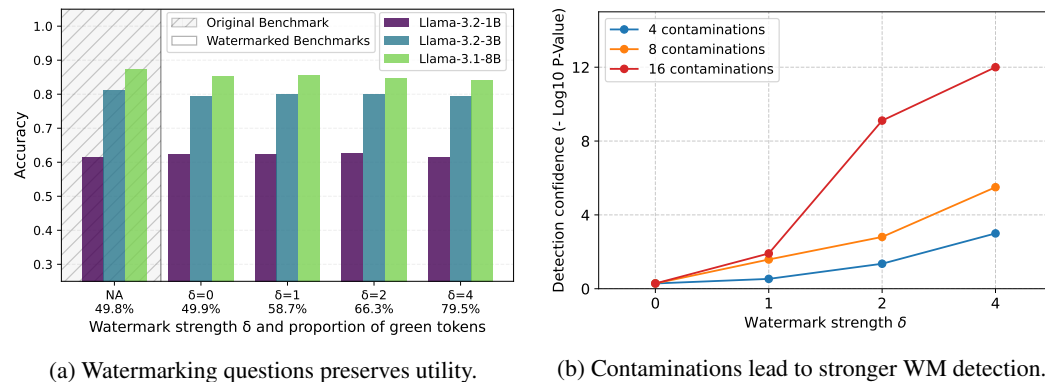


Figure 3: Result for benchmark watermarking on ARC-Easy. (Left) We rephrase the questions from ARC-Easy using Llama-3.1-8B-Instruct while adding watermarks of varying strength. The performance of multiple Llama-3 models on rephrased ARC-Easy is comparable to the original, preserving the benchmark’s usefulness for ranking models and assessing accuracy (Sec. 3.1, Sec. 4.1). (Right) We train 1B models from scratch on 10B tokens while intentionally contaminating its training set with the watermarked benchmark dataset. Increasing the number of contaminations and watermark strength both enhance detection confidence (Sec. 3.2, Sec. 4.2)

324
 325
 326
 327
 Table 1: Detection and performance metrics across different levels of contamination for ARC-Easy, ARC-
 Challenge, and MMLU benchmarks, watermarked with $\delta = 4$. The performance increase is shown for OOD
 evaluation as detailed in subsection 4.2. The $\log_{10} p$ -value of the detection test is strongly correlated with the
 number of contaminations, as well as with the performance increase of the LLM on the benchmark.

Contaminations	ARC-Easy (112k toks.)		ARC-Challenge (64k toks.)		MMLU* (325k toks.)	
	$\log_{10}(p)$	Acc. (% Δ)	$\log_{10}(p)$	Acc. (% Δ)	$\log_{10}(p)$	Acc. (% Δ)
0	-0.3	53.5 (+0.0)	-0.3	29.4 (+0.0)	-0.9	30.6 (+0.0)
4	-3.0	57.9 (+4.3)	-1.2	32.4 (+3.1)	-5.7	35.7 (+5.1)
8	-5.5	63.0 (+9.5)	-4.5	39.3 (+9.9)	<-12	40.8 (+10.2)
16	<-12	71.7 (+18.2)	<-12	54.3 (+24.9)	<-12	54.0 (+23.5)

334
 335
 336 number of contaminations (e.g. labels in Figure 3b): it corresponds to the number of times that the
 337 model has seen the benchmarks during pretraining.

338
 339 **Evaluation.** ARC and MMLU are multi-choice question-answering (QA) benchmarks. We evaluate
 340 the accuracy of the models on the benchmarks by comparing the loss between the different choices and
 341 choosing the one with the smallest loss (as standarly done in e.g. Gao et al. (2024)) either “in distri-
 342 bution” by using the above template seen during contamination or “out of distribution” (OOD)
 343 by using: f"During a lecture, the professor posed a question: {Question}.
 344 After discussion, it was revealed that the answer is: {Answer}"

345 In the first scenario, we evaluate overfitting, as the model is explicitly trained to minimize the loss of
 346 the correct answer within the same context. In the second scenario, we assess the model’s ability to
 347 confidently provide the answer in a slightly different context, which is more relevant for measuring
 348 contamination. Indeed, it’s important to note that evaluations often use templates around questions –
 349 e.g., in the lm-evaluation-harness library (Gao et al., 2024) – which may not be part of the
 350 question/answer files that could have leaked into the pre-training data. Table 1 focuses on $\delta = 4$ and
 351 shows the increase in performance across the three watermarked benchmarks as a function of the
 352 number of contaminations when evaluated OOD. Results for in-distribution evaluation are provided
 353 in Table 6 of Appendix A (w/o contamination, the model performs similarly on the two templates).

354 **Contamination detection.** For each benchmark, we employ the reading mode detailed in subsec-
 355 tion 3.2 to compute the radioactivity score S and the corresponding p -value. Results are illustrated
 356 in Figure 3b for ARC-Easy, and in Figure 8 of Appendix A for the other two benchmarks, across
 357 different numbers of contaminations and varying watermark strengths δ . We observe that the stronger
 358 the watermark strength and the greater the number of contaminations, the easier it is to detect contam-
 359 ination: a larger negative $\log_{10}(p)$ value indicates smaller p -values, implying a lower probability of
 360 obtaining this score if the model is not contaminated. For instance, a $-\log_{10}(p)$ of 6 implies that we
 361 can confidently assert model contamination, with a probability 10^{-6} of it happening by chance. We
 362 also observe that without contamination, the test yields $\log_{10}(p)$ values close to $-0.3 = \log_{10}(0.5)$.
 363 This is expected because under \mathcal{H}_0 , the p -value should follow a uniform distribution between 0 and 1,
 364 which implies that $[-1, 0]$ is a 90% confidence interval (CI) for $\log_{10}(p)$, and that $[-2, 0]$ is a 99% CI.

365 Table 1 links the contamination detection to the actual cheating on the benchmarks when $\delta = 4$ is
 366 used. For each benchmark column, the ‘Acc.’ sub-column shows the performance of the model at the
 367 end of training, for different numbers of contaminations. In light grey, we see how many percentage
 368 points the model has gained compared to the non-contaminated run. We can see that when the gain is
 369 around 10%, for all benchmarks, the corresponding p-value of the detection test is very small, and
 370 that we can therefore flag contamination with high confidence. When the cheat is smaller, with four
 371 contaminations ranging from +3% to +5%, the p -value is small enough on ARC-Easy and MMLU*,
 372 but doubtful for ARC-Challenge (because smaller, see subsection 4.4). For MMLU*, we detect
 373 contamination, with a p -value of 10^{-6} when 5 points are artificially added.

374 4.3 COMPARISON WITH OTHER CONTAMINATION DETECTION METHODS

375
 376 A variety of methods have been proposed to detect benchmark contamination. We categorize them
 377 as either *proactive* (requiring modification of the benchmark before release) or *post-hoc* (analyzing
 a model after training). Our work is proactive, providing verifiable guarantees, while most others

378 Table 2: Comparison of contamination detection methods. Post-hoc methods (*) which only provide **heuristics**
 379 evidence. **STAMP** (Rastogi et al., 2025) provides *p*-values, but can only be ran by the benchmark provider as
 380 it necessitates rephrased versions of the benchmark to be kept private. **Radioactive Benchmarks** and canaries
 381 provide *p*-values without necessitating held-out samples.

Method	Key Requirement	Evidence Type
Radioactive Benchmarks (Our Method)	Benchmark rephrasing	Statistical p-value
Canaries (Srivastava et al., 2022)	Canary string insertion	Statistical p-value
Min-k%/++* (Shi et al., 2023; Zhang et al., 2024b)	Logit access	Correlation
DyVal / KIEval* (Zhu et al., 2023; Yu et al., 2024)	Dynamic content	Performance delta
MIA* (Carlini et al., 2022; Maini et al., 2024)	Held-out set	Classifier score
STAMP (Rastogi et al., 2025)	Rephrasing + Held-out set	Statistical p-value

390 are post-hoc, offering strong but **heuristics** evidence. We always consider having logit access to the
 391 suspect models. Table 2 summarizes the key differences, which we discuss below.
 392

393 **Canaries.** Inserting “canaries” – unique, memorable strings – is another proactive method
 394 that provides theoretical guarantees, and has been used in benchmarks such as BIG-
 395 bench (Srivastava et al., 2022). We compare our approach to this important baseline.
 396 A random 64-digit string is added to one question of MMLU* and we pre-train a 360M-
 397 parameter model with 160 MMLU* contaminations, using the same set-up as for other exper-
 398 iments. We monitor memorization by forwarding
 399 the canary through the model and counting the
 400 number of correct digit predictions. A model
 401 that has not seen the canary guesses randomly,
 402 so the number of matches follows a binomial
 403 $B(64, 1/10)$. Table 3 demonstrates that even with 10 times more contamination than our most
 404 extreme setup, the model does not memorize the canary sufficiently to achieve a low *p*-value. This
 405 highlights the superior sensitivity of radioactivity, which distributes the signal across the entire text
 406 rather than concentrating it in one location that can be easily filtered or ignored during training.
 407

Table 3: 360M-parameter model sees a 64-digit canary
 160 times throughout the 10000 steps.

Training step	2500	5000	7500	10000
Matches	4/64	8/64	6/64	9/64
Loss	7.4	6.4	3.8	2.9
<i>p</i> -val	0.9	0.3	0.63	0.19

409 **Post-hoc methods.** A direct quantitative comparison with post-hoc methods is ill-suited, as they
 410 are fundamentally **heuristics** and often measure different phenomena than our proactive test. Among
 411 them, **Min-k%** (Shi et al., 2023) and its variants detect contamination by identifying text segments
 412 that elicit unusually low-loss values. While effective for general auditing, this provides correlational
 413 evidence of memorization, not the verifiable proof of exposure to a specific dataset that our secret-
 414 keyed watermark offers. Rewrite-based methods like DyVal (Zhu et al., 2023) and KIEval (Yu et al.,
 415 2024) address a different scientific question: they measure a model’s **capability to generalize** beyond
 416 memorized answers by creating dynamic evaluation samples. Their goal is to provide a contamination-
 417 resilient performance score, whereas our goal is to provide a *p*-value for contamination itself. As
 418 both papers acknowledge, their central challenge is validating the generated content’s quality and
 419 difficulty. Finally, we believe that classical **Membership Inference Attacks** (MIA*) (Carlini et al.,
 420 2022; Maini et al., 2024) are ill-suited for this problem, as they require a held-out set from the same
 421 distribution as the benchmark – a paradoxical requirement that, if met, would solve the contamination
 422 problem outright. Rastogi et al. (2025) approaches the problem differently by generating multiple
 423 watermarked rephrased versions of a benchmark: all are kept private except one. However, similar
 424 to other MIA*, contamination detection for STAMP is restricted to the entity holding the private
 425 benchmark versions. Therefore, because it necessitates open-weight (or at least grey-box) access
 426 to the model, it makes it impractical for evaluating proprietary models. Our proactive approach is
 427 designed to circumvent these limitations by providing a direct, verifiable test for data exposure.

428 4.4 ANALYZES

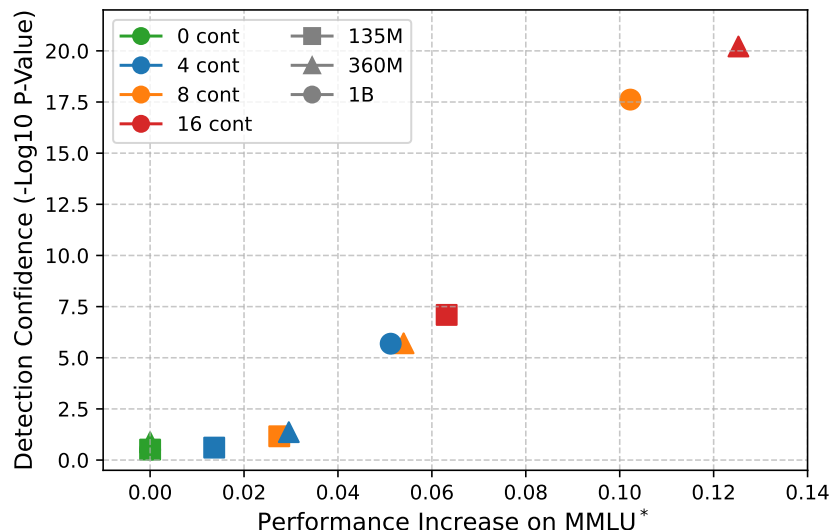
430 **Impact of model size.** We also test radioactivity detection on 135M and 360M transformer models
 431 using the architectures of SmolLM and the same training pipeline as described in subsection 4.2,
 training each model on 10B tokens as well. Figure 4 shows the detection confidence as a function

432 of the cheat on MMLU*. We find that, for a fixed number of contaminations, smaller models show
 433 less performance increase – expected as they memorize less – and we obtain lower confidence in the
 434 contamination detection test. As detailed in subsection 3.1, the p -values indicate how well a model
 435 overfits the questions, hence the expected correlation. For a fixed performance gain on benchmarks,
 436 p -values are consistent across models. After 4, 8, and 16 contaminations on the 1B, 360M, and
 437 135M models respectively, all models show around +6% gain, with detection tests yielding p -values
 438 around 10^{-5} . Thus, while larger models require fewer contaminations to achieve the same gain on the
 439 benchmark, our method effectively measures how contamination artificially enhanced performance.
 440

441 **Impact of window size.** Watermark insertion through
 442 rephrasing (subsection 3.1) depends on the watermark window
 443 size k . Each window creates a unique greenlist/redlist
 444 split for the next token. Larger windows reduce repeated
 445 biases but are less robust. Because of repetitions, Sander
 446 et al. (2024) show that smaller windows can lead to bigger
 447 overfitting on token-level watermark biases, helping
 448 radioactivity detection. In our case, benchmark sizes are
 449 relatively small and deduplication limits the number of to-
 450 kens tested, because each watermarked window is scored
 451 only once (subsection 3.2). Thus, smaller windows mean
 452 fewer tokens to score. Moreover, as shown in Table 4, the proportion of predicted green tokens
 453 is not even larger for smaller windows: there seems to be not enough repetitions for increased
 454 over-fitting on smaller windows. The two factors combined result in lower confidence. A comparison
 455 of contamination detection across benchmarks and window sizes is shown in Figure 7, and the utility
 456 of the benchmarks in Figure 8.

457 **Impact of benchmark size.** With a fixed proportion of predicted green tokens, more evidence (*i.e.*,
 458 more scored tokens) increases test confidence. As shown in Table 1, at a fixed level of cheating (*e.g.*,
 459 +10% on all benchmarks after 8 contaminations), contamination detection confidence is proportional
 460 to benchmark size. This is similar to our observations on watermark window sizes in Table 4.

461 **Impact of rephrasing model.** The difficulty and entropy of questions can significantly affect the
 462 method’s performance. Indeed, math questions for instance can be challenging to rephrase, even
 463 more with watermarks. Thus, better models may be needed for technical benchmarks. We tested
 464 rephrasing with Llama3-70B-Instruct instead of the 8B version, and observed that some 8B model
 465 failures, especially on mathy questions, are resolved with the 70B model, though quantifying this is
 466
 467



484 Figure 4: Detection confidence as a function of performance increase on MMLU* for different model sizes and
 485 #contaminations, for $\delta = 4$ and OOD evaluation.

Table 4: Proportion of green tokens in the predictions, number of tokens scored after deduplication and $\log_{10}(p\text{-value})$ for different watermark window sizes, with 16 contaminations and $\delta = 4$ on ARC-Easy.

k	ρ	Tokens	$\log_{10}(p)$
0	0.53	5k	-6.07
1	0.53	28k	-25.89
2	0.53	47k	-38.69

486
 487 Table 5: Performance and contamination detection when pretraining models with fixed backbone architecture
 488 from scratch on 10B tokens with different tokenizers, with and without 16 contamination of MMLU*, water-
 489 marked with $\delta = 4$ using Llama-3’s tokenizer. The gray line highlights that this is the ideal case were both
 490 tokenizers match, as in previous sections. We use our new algorithm 1 for the contamination detection test.

Tokenizer	Vocab Size	#Params (in millions)	#Tokens Scored (in thousands)	w/ Contamination $\log_{10}(p)$	Acc.	w/o Contamination $\log_{10}(p)$	Acc.
Llama-1/2	32K	376	149 (44.9%)	-7	39.1	-0.1	27.4
Gemma-1/2	256K	806	142 (42.8%)	-12	44.3	-0.2	30.1
Gemma-3	262K	818	142 (42.9%)	-15	44.5	-0.1	30.3
Llama-3	128K	561	154 (46.4%)	-14	41.2	-0.6	29.6

491
 492 challenging. An example is provided in Figure 6 of app. A. We note that increasing δ to 8 is necessary
 493 to match the green token proportion of $\delta = 2$ with the 8B model, using the same decoding parameters.
 494 This may result from lower entropy in generation or bigger logits, as the greenlist bias is applied
 495 before the softmax (see subsection 3.1). Moreover, in math or code, rephrasing can offer limited
 496 entropy, and even better models will not be enough. An alternative would be to add watermarked
 497 verbose text *around* the questions, or using entropy-aware LLM watermarking (Lee et al., 2023).

504 4.5 DIFFERENCE IN TOKENIZERS

505 In section 4.2 and section 4.4, the tokenizer of Llama-3 was used for both the watermark embedding
 506 and by the suspect model. Using algorithm 1, we show here that contamination detection remains
 507 strong and reliable when another tokenizer is used by the suspect model. We keep the tokenizer of
 508 Llama-3 for watermark embedding, and use the tokenizers of Llama-1/2 (Touvron et al., 2023a;b),
 509 Llama-3, Gemma-1/2 (Team et al., 2024b;a), Gemma-3 (Team et al., 2025) for the suspect model.

510 Table 5 presents the performance metrics and contamination detection capabilities of models pre-
 511 trained with various tokenizers, both with and without contamination on MMLU*, with 16 contami-
 512 nations, and $\delta = 4$. The vocabulary size affects the number of parameters in the model, impacting
 513 both the embedding and output layers, as highlighted in the “#Params” column. First, we observe
 514 that the test remains reliable, as indicated by small p -values in the absence of contamination. Second,
 515 the “#Tokens Scored” column shows that scoring only tokens shared across vocabularies (the trigger
 516 condition in our Algorithm 1) still results in a substantial number of tokens being scored. This results
 517 in high detection confidence across all tokenizers. However, we note that the test appears weaker for
 518 Llama-1’s tokenizer. This might be due to the corresponding model having fewer parameters, making
 519 it less prone to memorizing the watermark, but this is not because fewer tokens are scored.

521 5 LIMITATIONS & CONCLUSION

- 522 • **Rephrasing impact:** Model performance remains similar across benchmark versions, but some
 523 questions lose coherence after rephrasing (e.g., Figure 6), which can be difficult to spot. Possible
 524 improvements are discussed in subsection 3.1 and subsection 4.4.
- 525 • **Intentional evasion:** The method is primarily designed for unintentional contamination. Malicious
 526 actors could rephrase questions to weaken the watermark or train only on answers conditioned on
 527 questions, which would bypass radioactivity detection.
- 528 • **Before release:** The method is only applicable to protect new datasets, not existing ones.

529
 530 **Conclusion.** Watermarking benchmark appears like a promising solution to the problem of contam-
 531 ination in Large Language Models: experiments confirm the method’s ability to maintain benchmark
 532 utility while successfully identifying contamination. We note that the method can be applied to other
 533 text datasets: the statistical test’s power depends on the number of watermarked tokens the model has
 534 memorized, making it a general solution for any textual dataset used, in pretraining or finetuning.

535
 536 **Statement on LLM Usage:** We used LLMs to polish the writing of some parts of the paper. We
 537 also used LLM-based tools to check if we had missed relevant related work.

540 REFERENCES
541

542 Scott Aaronson and Hendrik Kirchner. Watermarking GPT outputs, 2023. URL <https://scottaaronson.blog/?m=202302>.

543

544 Jinze Bai, Shuai Bai, Yunfei Chu, Zeyu Cui, Kai Dang, Xiaodong Deng, Yang Fan, Wenbin Ge,
545 Yu Han, Fei Huang, et al. Qwen technical report. *arXiv preprint arXiv:2309.16609*, 2023.

546

547 Simone Balloccu, Patrícia Schmidlová, Mateusz Lango, and Ondřej Dušek. Leak, cheat, repeat: Data
548 contamination and evaluation malpractices in closed-source llms. *arXiv preprint arXiv:2402.03927*,
549 2024.

550

551 Tom Brown, Benjamin Mann, Nick Ryder, Melanie Subbiah, Jared D Kaplan, Prafulla Dhariwal,
552 Arvind Neelakantan, Pranav Shyam, Girish Sastry, Amanda Askell, et al. Language models are
553 few-shot learners. *Advances in neural information processing systems*, 33:1877–1901, 2020.

554

555 Nicholas Carlini, Daphne Ippolito, Matthew Jagielski, Katherine Lee, Florian Tramer, and
556 Chiyuan Zhang. Quantifying memorization across neural language models. *arXiv preprint
arXiv:2202.07646*, 2022.

557

558 Miranda Christ, Sam Gunn, and Or Zamir. Undetectable watermarks for language models. *Cryptology
ePrint Archive*, 2023.

559

560 Peter Clark, Isaac Cowhey, Oren Etzioni, Tushar Khot, Ashish Sabharwal, Carissa Schoenick, and
561 Oyyvind Tafjord. Think you have solved question answering? try arc, the ai2 reasoning challenge.
562 *arXiv preprint arXiv:1803.05457*, 2018.

563

564 Karl Cobbe, Vineet Kosaraju, Mohammad Bavarian, Mark Chen, Heewoo Jun, Lukasz Kaiser,
565 Matthias Plappert, Jerry Tworek, Jacob Hilton, Reiichiro Nakano, et al. Training verifiers to solve
566 math word problems. *arXiv preprint arXiv:2110.14168*, 2021.

567

568 Yihe Deng, Weitong Zhang, Zixiang Chen, and Quanquan Gu. Rephrase and respond: Let large
569 language models ask better questions for themselves. *arXiv preprint arXiv:2311.04205*, 2023.

570

571 André V. Duarte, Xuandong Zhao, Arlindo L. Oliveira, and Lei Li. De-cop: Detecting copyrighted
572 content in language models training data, 2024. URL <https://arxiv.org/abs/2402.09910>.

573

574 Abhimanyu Dubey, Abhinav Jauhri, Abhinav Pandey, Abhishek Kadian, Ahmad Al-Dahle, Aiesha
575 Letman, Akhil Mathur, Alan Schelten, Amy Yang, Angela Fan, et al. The llama 3 herd of models.
576 *arXiv preprint arXiv:2407.21783*, 2024.

577

578 Fay Elhassan, Niccolò Ajroldi, Antonio Orvieto, and Jonas Geiping. Can you finetune your binoc-
579 ulars? embedding text watermarks into the weights of large language models. *arXiv preprint
arXiv:2504.06446*, 2025.

580

581 Angela Fan, Mike Lewis, and Yann Dauphin. Hierarchical neural story generation. *arXiv preprint
arXiv:1805.04833*, 2018.

582

583 Pierre Fernandez, Antoine Chaffin, Karim Tit, Vivien Chappelier, and Teddy Furon. Three bricks
584 to consolidate watermarks for large language models. *2023 IEEE International Workshop on
585 Information Forensics and Security (WIFS)*, 2023.

586

587 Yu Fu, Deyi Xiong, and Yue Dong. Watermarking conditional text generation for ai detection:
588 Unveiling challenges and a semantic-aware watermark remedy. In *Proceedings of the AAAI
589 Conference on Artificial Intelligence*, 2024.

590

591 Leo Gao, Jonathan Tow, Baber Abbasi, Stella Biderman, Sid Black, Anthony DiPofi, Charles Foster,
592 Laurence Golding, Jeffrey Hsu, Alain Le Noac'h, Haonan Li, Kyle McDonell, Niklas Muennighoff,
593 Chris Ociepa, Jason Phang, Laria Reynolds, Hailey Schoelkopf, Aviya Skowron, Lintang Sutawika,
Eric Tang, Anish Thite, Ben Wang, Kevin Wang, and Andy Zou. A framework for few-shot
language model evaluation, 07 2024. URL <https://zenodo.org/records/12608602>.

594 Elliot Glazer, Ege Erdil, Tamay Besiroglu, Diego Chicharro, Evan Chen, Alex Gunning, Caroline Falk-
 595 man Olsson, Jean-Stanislas Denain, Anson Ho, Emily de Oliveira Santos, et al. Frontiermath: A
 596 benchmark for evaluating advanced mathematical reasoning in ai. *arXiv preprint arXiv:2411.04872*,
 597 2024.

598 Thibaud Gloaguen, Nikola Jovanović, Robin Staab, and Martin Vechev. Towards watermarking of
 599 open-source llms. *arXiv preprint arXiv:2502.10525*, 2025.

601 Aaron Grattafiori, Abhimanyu Dubey, Abhinav Jauhri, Abhinav Pandey, Abhishek Kadian, Ahmad
 602 Al-Dahle, Aiesha Letman, Akhil Mathur, Alan Schelten, Alex Vaughan, et al. The llama 3 herd of
 603 models. *arXiv preprint arXiv:2407.21783*, 2024.

604 Chenchen Gu, Xiang Lisa Li, Percy Liang, and Tatsunori Hashimoto. On the learnability of water-
 605 marks for language models. *arXiv preprint arXiv:2312.04469*, 2023.

607 Dan Hendrycks, Collin Burns, Steven Basart, Andy Zou, Mantas Mazeika, Dawn Song, and
 608 Jacob Steinhardt. Measuring massive multitask language understanding. *arXiv preprint*
 609 *arXiv:2009.03300*, 2020.

611 Ari Holtzman, Jan Buys, Li Du, Maxwell Forbes, and Yejin Choi. The curious case of neural text
 612 degeneration. *arXiv preprint arXiv:1904.09751*, 2019.

613 Baihe Huang, Banghua Zhu, Hanlin Zhu, Jason D. Lee, Jiantao Jiao, and Michael I. Jordan. Towards
 614 optimal statistical watermarking, 2023.

616 Minhao Jiang, Ken Ziyu Liu, Ming Zhong, Rylan Schaeffer, Siru Ouyang, Jiawei Han, and Sanmi
 617 Koyejo. Investigating data contamination for pre-training language models. *arXiv preprint*
 618 *arXiv:2401.06059*, 2024.

619 Nikola Jovanović, Robin Staab, Maximilian Baader, and Martin Vechev. Ward: Provable rag dataset
 620 inference via llm watermarks. *arXiv preprint arXiv:2410.03537*, 2024.

622 John Kirchenbauer, Jonas Geiping, Yuxin Wen, Jonathan Katz, Ian Miers, and Tom Goldstein. A
 623 watermark for large language models. *arXiv preprint arXiv:2301.10226*, 2023a.

625 John Kirchenbauer, Jonas Geiping, Yuxin Wen, Manli Shu, Khalid Saifullah, Kezhi Kong, Kasun
 626 Fernando, Amiruddha Saha, Micah Goldblum, and Tom Goldstein. On the reliability of watermarks
 627 for large language models, 2023b.

628 Rohith Kuditipudi, John Thickstun, Tatsunori Hashimoto, and Percy Liang. Robust distortion-free
 629 watermarks for language models. *arXiv preprint arXiv:2307.15593*, 2023.

631 Taehyun Lee, Seokhee Hong, Jaewoo Ahn, Ilgee Hong, Hwaran Lee, Sangdoo Yun, Jamin Shin,
 632 and Gunhee Kim. Who wrote this code? watermarking for code generation. *arXiv preprint*
 633 *arXiv:2305.15060*, 2023.

634 Jeffrey Li, Alex Fang, Georgios Smyrnis, Maor Ivgi, Matt Jordan, Samir Gadre, Hritik Bansal, Etash
 635 Guha, Sedrick Keh, Kushal Arora, et al. Datacomp-lm: In search of the next generation of training
 636 sets for language models. *arXiv preprint arXiv:2406.11794*, 2024.

638 Aiwei Liu, Leyi Pan, Xuming Hu, Shiao Meng, and Lijie Wen. A semantic invariant robust watermark
 639 for large language models. *arXiv preprint arXiv:2310.06356*, 2023.

640 Peter J. Liu, Mohammad Saleh, Etienne Pot, Ben Goodrich, Ryan Sepassi, Lukasz Kaiser, and
 641 Noam Shazeer. Generating wikipedia by summarizing long sequences, 2018. URL <https://arxiv.org/abs/1801.10198>.

644 Yepeng Liu and Yuheng Bu. Adaptive text watermark for large language models. *arXiv preprint*
 645 *arXiv:2401.13927*, 2024.

646 Pratyush Maini, Hengrui Jia, Nicolas Papernot, and Adam Dziedzic. Llm dataset inference: Did you
 647 train on my dataset?, 2024. URL <https://arxiv.org/abs/2406.06443>.

648 Matthieu Meeus, Igor Shilov, Shubham Jain, Manuel Faysse, Marek Rei, and Yves-Alexandre
 649 de Montjoye. Sok: Membership inference attacks on llms are rushing nowhere (and how to fix it).
 650 In *2025 IEEE Conference on Secure and Trustworthy Machine Learning (SaTML)*, pp. 385–401.
 651 IEEE, 2025.

652 Yonatan Oren, Nicole Meister, Niladri Chatterji, Faisal Ladakh, and Tatsunori B. Hashimoto. Proving
 653 test set contamination in black box language models, 2023. URL <https://arxiv.org/abs/2310.17623>.

654 Alec Radford and Karthik Narasimhan. Improving language understanding by generative pre-training.
 655 2018. URL <https://api.semanticscholar.org/CorpusID:49313245>.

656 Saksham Rastogi, Pratyush Maini, and Danish Pruthi. Stamp your content: Proving dataset member-
 657 ship via watermarked rephrasings, 2025. URL <https://arxiv.org/abs/2504.13416>.

658 David Rein, Betty Li Hou, Asa Cooper Stickland, Jackson Petty, Richard Yuanzhe Pang, Julien Dirani,
 659 Julian Michael, and Samuel R Bowman. Gpqa: A graduate-level google-proof q&a benchmark.
 660 *arXiv preprint arXiv:2311.12022*, 2023.

661 Alexandre Sablayrolles, Matthijs Douze, Cordelia Schmid, and Hervé Jégou. Radioactive data:
 662 tracing through training. In *International Conference on Machine Learning*, pp. 8326–8335.
 663 PMLR, 2020.

664 Tom Sander, Pierre Fernandez, Alain Durmus, Matthijs Douze, and Teddy Furon. Watermarking
 665 makes language models radioactive. *arXiv preprint arXiv:2402.14904*, 2024.

666 Weijia Shi, Anirudh Ajith, Mengzhou Xia, Yangsibo Huang, Daogao Liu, Terra Blevins, Danqi Chen,
 667 and Luke Zettlemoyer. Detecting pretraining data from large language models. *arXiv preprint
 668 arXiv:2310.16789*, 2023.

669 Aaditya K Singh, Muhammed Yusuf Kocyigit, Andrew Poulton, David Esiobu, Maria Lomeli, Gergely
 670 Szilvassy, and Dieuwke Hupkes. Evaluation data contamination in llms: how do we measure it and
 671 (when) does it matter? *arXiv preprint arXiv:2411.03923*, 2024.

672 Aarohi Srivastava, Abhinav Rastogi, Abhishek Rao, Abu Awal Md Shoeb, Abubakar Abid, Adam
 673 Fisch, Adam R Brown, Adam Santoro, Aditya Gupta, Adrià Garriga-Alonso, et al. Beyond the
 674 imitation game: Quantifying and extrapolating the capabilities of language models. *arXiv preprint
 675 arXiv:2206.04615*, 2022.

676 Gemma Team, Thomas Mesnard, Cassidy Hardin, Robert Dadashi, Surya Bhupatiraju, Shreya Pathak,
 677 Laurent Sifre, Morgane Rivière, Mihir Sanjay Kale, Juliette Love, et al. Gemma: Open models
 678 based on gemini research and technology. *arXiv preprint arXiv:2403.08295*, 2024a.

679 Gemma Team, Morgane Riviere, Shreya Pathak, Pier Giuseppe Sessa, Cassidy Hardin, Surya
 680 Bhupatiraju, Léonard Hussenot, Thomas Mesnard, Bobak Shahriari, Alexandre Ramé, et al.
 681 Gemma 2: Improving open language models at a practical size. *arXiv preprint arXiv:2408.00118*,
 682 2024b.

683 Gemma Team, Aishwarya Kamath, Johan Ferret, Shreya Pathak, Nino Vieillard, Ramona Merhej,
 684 Sarah Perrin, Tatiana Matejovicova, Alexandre Ramé, Morgane Rivière, et al. Gemma 3 technical
 685 report. *arXiv preprint arXiv:2503.19786*, 2025.

686 Hugo Touvron, Thibaut Lavril, Gautier Izacard, Xavier Martinet, Marie-Anne Lachaux, Timothée
 687 Lacroix, Baptiste Rozière, Naman Goyal, Eric Hambr, Faisal Azhar, et al. Llama: Open and
 688 efficient foundation language models. *arXiv preprint arXiv:2302.13971*, 2023a.

689 Hugo Touvron, Louis Martin, Kevin Stone, Peter Albert, Amjad Almahairi, Yasmine Babaei, Nikolay
 690 Bashlykov, Soumya Batra, Prajjwal Bhargava, Shruti Bhosale, et al. Llama 2: Open foundation
 691 and fine-tuned chat models. *arXiv preprint arXiv:2307.09288*, 2023b.

692 Ashish Vaswani, Noam Shazeer, Niki Parmar, Jakob Uszkoreit, Llion Jones, Aidan N Gomez, Łukasz
 693 Kaiser, and Illia Polosukhin. Attention is all you need. *Advances in neural information processing
 694 systems*, 30, 2017.

702 Mathurin Videau, Badr Youbi Idrissi, Daniel Haziza, Luca Wehrstedt, Jade Copet, Olivier Teytaud,
 703 and David Lopez-Paz. Meta Lingua: A minimal PyTorch LLM training library, 2024. URL
 704 <https://github.com/facebookresearch/lingua>.

705

706 Shuo Yang, Wei-Lin Chiang, Lianmin Zheng, Joseph E Gonzalez, and Ion Stoica. Rethinking
 707 benchmark and contamination for language models with rephrased samples. *arXiv preprint*
 708 *arXiv:2311.04850*, 2023.

709

710 Zhuohao Yu, Chang Gao, Wenjin Yao, Yidong Wang, Wei Ye, Jindong Wang, Xing Xie, Yue Zhang,
 711 and Shikun Zhang. Kieval: A knowledge-grounded interactive evaluation framework for large
 712 language models. *arXiv preprint arXiv:2402.15043*, 2024.

713

714 Hugh Zhang, Jeff Da, Dean Lee, Vaughn Robinson, Catherine Wu, Will Song, Tiffany Zhao, Pranav
 715 Raja, Dylan Slack, Qin Lyu, et al. A careful examination of large language model performance on
 716 grade school arithmetic. *arXiv preprint arXiv:2405.00332*, 2024a.

717

718 Jingyang Zhang, Jingwei Sun, Eric Yeats, Yang Ouyang, Martin Kuo, Jianyi Zhang, Hao Frank Yang,
 719 and Hai Li. Min-k%++: Improved baseline for detecting pre-training data from large language
 720 models. *arXiv preprint arXiv:2404.02936*, 2024b.

721

722 Xuandong Zhao, Yu-Xiang Wang, and Lei Li. Protecting language generation models via invisible
 723 watermarking. In *International Conference on Machine Learning*, pp. 42187–42199. PMLR, 2023.

724

725

726

727

728

729

730

731

732

733

734

735

736

737

738

739

740

741

742

743

744

745

746

747

748

749

750

751

752

753

754

755

756 **A ADDITIONAL EXPERIMENTS**
757758 **A.1 QUALITATIVE EXAMPLES**
759760 On one question from ARC-Easy, we compare qualitatively different watermarking strengths in Figure 5. We also show failure cases in fig. 6, but where rephrasing with the 70B model works.
761762 **A.2 ADDITIONAL EXPERIMENTAL RESULTS**
763764 **Evaluation Template.** As detailed in subsection 4.2, we evaluate the accuracy on the benchmark
765 using both the same template seen during contamination and an alternative one. Table 6 presents the
766 results when evaluated with the same template. Without contamination, the model performs similarly
767 across the two templates, but a differences appear with contaminations.
768769 **Ablations on different benchmarks, watermark strength, watermark window sizes, and number**
770 **of contaminations.** Results for all benchmarks (ARC-Easy, ARC-Challenge, and MMLU*), with
771 variations in watermark window size, number of contaminations, and watermark strength, are shown
772 in Figure 7 for utility and Figure 8 for radioactivity detection. For utility, all models perform very
773 similarly on all the rephrased versions of the benchmarks, even when pushing the watermark to
774 80% of green tokens, although for MMLU*, we observe some discrepancies. For instance, when
775 using a watermarking window size of 2 (subfig i), the performance of Llama-3.2-1B increases from
776 38% to 42% between the original and the other versions. However we observe the same issue when
777 rephrasing without watermarking in that case. The watermark window size does not have an impact.
778 For radioactivity detection on the other hand, as detailed in subsection 4.4, smaller window sizes
779 correlates with lower detection confidence.
780781
782
783
784 **System Prompt:** “You are a problem rephrasing
785 assistant. Your task is to rephrase the given prob-
786 lem, which includes a question, while ensuring
787 that the rephrased version is logically and context-
788 ually equivalent to the original. Do not provide
789 answers or solutions to the problem.”790 **Instruction:** “Please rephrase the following prob-
791 lem, ensuring that the rephrased version is equiva-
792 lent to the original in terms of logic, context, and
793 details. Your response should only include the
794 rephrased version of the problem and question.
Beginning of the problem:”795 **Question:** “The rate of acceleration of an object
796 is determined by the mass of the object and”797
800 **Llama-3-8B-Instruct Rephrased, $\delta = 0$**
801 What factors, in addition to the mass of an object,
802 influence its rate of acceleration? (47%)803 **Llama-3-8B-Instruct Rephrased, $\delta = 0.5$**
804 What factor, in addition to the mass of an ob-
805 ject, influences the rate at which its acceleration
806 changes over time? (55%)807 **Llama-3-8B-Instruct Rephrased, $\delta = 2$**
808 What factor, in addition to the mass of an object,
809 is a determining influence on its rate of accelera-
810 tion? (63%)811 **Llama-3-8B-Instruct Rephrased, $\delta = 4$**
812 What factor, aside from an object’s mass, deter-
813 mines its acceleration? (73%)814
815
816
817
818
819
820
821
822
823
824
825
826
827
828
829
830
831
832
833
834
835
836
837
838
839
840
841
842
843
844
845
846
847
848
849
850
851
852
853
854
855
856
857
858
859
860
861
862
863
864
865
866
867
868
869
870
871
872
873
874
875
876
877
878
879
880
881
882
883
884
885
886
887
888
889
890
891
892
893
894
895
896
897
898
899
900
901
902
903
904
905
906
907
908
909
910
911
912
913
914
915
916
917
918
919
920
921
922
923
924
925
926
927
928
929
930
931
932
933
934
935
936
937
938
939
940
941
942
943
944
945
946
947
948
949
950
951
952
953
954
955
956
957
958
959
960
961
962
963
964
965
966
967
968
969
970
971
972
973
974
975
976
977
978
979
980
981
982
983
984
985
986
987
988
989
990
991
992
993
994
995
996
997
998
999
1000
1001
1002
1003
1004
1005
1006
1007
1008
1009
1010
1011
1012
1013
1014
1015
1016
1017
1018
1019
1020
1021
1022
1023
1024
1025
1026
1027
1028
1029
1030
1031
1032
1033
1034
1035
1036
1037
1038
1039
1040
1041
1042
1043
1044
1045
1046
1047
1048
1049
1050
1051
1052
1053
1054
1055
1056
1057
1058
1059
1060
1061
1062
1063
1064
1065
1066
1067
1068
1069
1070
1071
1072
1073
1074
1075
1076
1077
1078
1079
1080
1081
1082
1083
1084
1085
1086
1087
1088
1089
1090
1091
1092
1093
1094
1095
1096
1097
1098
1099
1100
1101
1102
1103
1104
1105
1106
1107
1108
1109
1110
1111
1112
1113
1114
1115
1116
1117
1118
1119
1120
1121
1122
1123
1124
1125
1126
1127
1128
1129
1130
1131
1132
1133
1134
1135
1136
1137
1138
1139
1140
1141
1142
1143
1144
1145
1146
1147
1148
1149
1150
1151
1152
1153
1154
1155
1156
1157
1158
1159
1160
1161
1162
1163
1164
1165
1166
1167
1168
1169
1170
1171
1172
1173
1174
1175
1176
1177
1178
1179
1180
1181
1182
1183
1184
1185
1186
1187
1188
1189
1190
1191
1192
1193
1194
1195
1196
1197
1198
1199
1200
1201
1202
1203
1204
1205
1206
1207
1208
1209
1210
1211
1212
1213
1214
1215
1216
1217
1218
1219
1220
1221
1222
1223
1224
1225
1226
1227
1228
1229
1230
1231
1232
1233
1234
1235
1236
1237
1238
1239
1240
1241
1242
1243
1244
1245
1246
1247
1248
1249
1250
1251
1252
1253
1254
1255
1256
1257
1258
1259
1260
1261
1262
1263
1264
1265
1266
1267
1268
1269
1270
1271
1272
1273
1274
1275
1276
1277
1278
1279
1280
1281
1282
1283
1284
1285
1286
1287
1288
1289
1290
1291
1292
1293
1294
1295
1296
1297
1298
1299
1300
1301
1302
1303
1304
1305
1306
1307
1308
1309
1310
1311
1312
1313
1314
1315
1316
1317
1318
1319
1320
1321
1322
1323
1324
1325
1326
1327
1328
1329
1330
1331
1332
1333
1334
1335
1336
1337
1338
1339
1340
1341
1342
1343
1344
1345
1346
1347
1348
1349
1350
1351
1352
1353
1354
1355
1356
1357
1358
1359
1360
1361
1362
1363
1364
1365
1366
1367
1368
1369
1370
1371
1372
1373
1374
1375
1376
1377
1378
1379
1380
1381
1382
1383
1384
1385
1386
1387
1388
1389
1390
1391
1392
1393
1394
1395
1396
1397
1398
1399
1400
1401
1402
1403
1404
1405
1406
1407
1408
1409
1410
1411
1412
1413
1414
1415
1416
1417
1418
1419
1420
1421
1422
1423
1424
1425
1426
1427
1428
1429
1430
1431
1432
1433
1434
1435
1436
1437
1438
1439
1440
1441
1442
1443
1444
1445
1446
1447
1448
1449
1450
1451
1452
1453
1454
1455
1456
1457
1458
1459
1460
1461
1462
1463
1464
1465
1466
1467
1468
1469
1470
1471
1472
1473
1474
1475
1476
1477
1478
1479
1480
1481
1482
1483
1484
1485
1486
1487
1488
1489
1490
1491
1492
1493
1494
1495
1496
1497
1498
1499
1500
1501
1502
1503
1504
1505
1506
1507
1508
1509
1510
1511
1512
1513
1514
1515
1516
1517
1518
1519
1520
1521
1522
1523
1524
1525
1526
1527
1528
1529
1530
1531
1532
1533
1534
1535
1536
1537
1538
1539
1540
1541
1542
1543
1544
1545
1546
1547
1548
1549
1550
1551
1552
1553
1554
1555
1556
1557
1558
1559
1560
1561
1562
1563
1564
1565
1566
1567
1568
1569
1570
1571
1572
1573
1574
1575
1576
1577
1578
1579
1580
1581
1582
1583
1584
1585
1586
1587
1588
1589
1590
1591
1592
1593
1594
1595
1596
1597
1598
1599
1600
1601
1602
1603
1604
1605
1606
1607
1608
1609
1610
1611
1612
1613
1614
1615
1616
1617
1618
1619
1620
1621
1622
1623
1624
1625
1626
1627
1628
1629
1630
1631
1632
1633
1634
1635
1636
1637
1638
1639
1640
1641
1642
1643
1644
1645
1646
1647
1648
1649
1650
1651
1652
1653
1654
1655
1656
1657
1658
1659
1660
1661
1662
1663
1664
1665
1666
1667
1668
1669
1670
1671
1672
1673
1674
1675
1676
1677
1678
1679
1680
1681
1682
1683
1684
1685
1686
1687
1688
1689
1690
1691
1692
1693
1694
1695
1696
1697
1698
1699
1700
1701
1702
1703
1704
1705
1706
1707
1708
1709
17010
17011
17012
17013
17014
17015
17016
17017
17018
17019
17020
17021
17022
17023
17024
17025
17026
17027
17028
17029
17030
17031
17032
17033
17034
17035
17036
17037
17038
17039
17040
17041
17042
17043
17044
17045
17046
17047
17048
17049
17050
17051
17052
17053
17054
17055
17056
17057
17058
17059
17060
17061
17062
17063
17064
17065
17066
17067
17068
17069
17070
17071
17072
17073
17074
17075
17076
17077
17078
17079
17080
17081
17082
17083
17084
17085
17086
17087
17088
17089
17090
17091
17092
17093
17094
17095
17096
17097
17098
17099
170100
170101
170102
170103
170104
170105
170106
170107
170108
170109
170110
170111
170112
170113
170114
170115
170116
170117
170118
170119
170120
170121
170122
170123
170124
170125
170126
170127
170128
170129
170130
170131
170132
170133
170134
170135
170136
170137
170138
170139
170140
170141
170142
170143
170144
170145
170146
170147
170148
170149
170150
170151
170152
170153
170154
170155
170156
170157
170158
170159
170160
170161
170162
170163
170164
170165
170166
170167
170168
170169
170170
170171
170172
170173
170174
170175
170176
170177
170178
170179
170180
170181
170182
170183
170184
170185
170186
170187
170188
170189
170190
170191
170192
170193
170194
170195
170196
170197
170198
170199
170200
170201
170202
170203
170204
170205
170206
170207
170208
170209
170210
170211
170212
170213
170214
170215
170216
170217
170218
170219
170220
170221
170222
170223
170224
170225
170226
170227
170228
170229
170230
170231
170232
170233
170234
170235
170236
170237
170238
170239
170240
170241
170242
170243
170244
170245
170246
170247
170248
170249
170250
170251
170252
170253
170254
170255
170256
170257
170258
170259
170260
170261
170262
170263
170264
170265
170266
170267
170268
170269
170270
170271
170272
170273
170274
170275
170276
170277
170278
170279
170280
170281
170282
170283
170284
170285
170286
170287
170288
170289
170290
170291
170292
170293
170294
170295
170296
170297
170298
170299
170300
170301
170302
170303
170304
170305
170306
170307
170308
170309
170310
170311
170312
170313
170314
170315
170316
170317
170318
170319
170320
170321
170322
170323
170324
170325
170326
170327
170328
170329
170330
170331
170332
170333
170334
170335
170336
170337
170338
170339
170340
170341
170342
170343
170344
170345
170346
170347
170348
170349
170350
170351
170352
170353
170354
170355
170356
170357
170358
170359
170360
170361
170362
170363
170364
170365
170366
170367
170368
170369
170370
170371
170372
170373
170374
170375
170376
170377
170378
170379
170380
170381
170382
170383
170384
170385
170386
170387
170388
170389
170390
170391
170392
170393
170394
170395
170396
170397
170398
170399
170400
170401
170402
170403
170404
170405
170406
170407
170408
170409
170410
170411
170412
170413
170414
170415
170416
170417
170418
170419
170420
170421
170422
170423
170424
170425
170426
170427
170428
170429
170430
170431
170432
170433
170434
170435
170436
170437
170438
170439
170440
170441
170442
170443
170444
170445
170446
170447
170448
170449
170450
170451
170452
170453
170454
170455
170456
170457
170458
170459
170460
170461
170462
170463
170464
170465
170466
170467
170468
170469
170470
170471
170472
170473
170474
170475
170476
170477
170478
170479
170480
170481
170482
170483
170484
170485
170486
170487
170488
170489
170490
170491
170492
170493
170494
170495
170496
170497
170498
170499
170500
170501
170502
170503
170504
170505
170506
170507
170508
170509
170510
170511
170512
170513
170514
170515
170516
170517
170518
170519
170520
170521
170522
170523
170524
170525
170526
170527
170528
170529
170530
170531
170532
170533
170534
170535
170536
170537
170538
170539
170540
170541
170542
170543
170544
170545
170546
170547
170548
170549
170550
170551
170552
170553
170554
170555
170556
170557
170558
170559
170560
170561
170562
170563
170564
170565
170566
170567
170568
170569
170570
170571
170572
170573
170574
170575
170576
170577
170578
170579
170580
170581
170582
170583
170584
170585
170586
170587
170588
170589
170590
170591
170592
170593
170594
170595
170596
170597
170598
170599
170600
170601
170602
170603
170604
170605
170606
170607
170608
170609
170610
170611
170612

810
811
812
813
814
815
816
817
818
819
820
821
822
823
824
825
826
827
828
829
830
831
832
833
834
835
836
837
838
839
840
841
842
843
844
845
846
847
848
849
850
851
852
853
854
855
856
857
858
859
860
861
862
863

Table 6: Detection and performance metrics across different levels of contamination for ARC-Easy, ARC-Challenge, and MMLU benchmarks, watermarked with $\delta = 4$. The performance increase is for in distribution evaluation as detailed in subsection 4.2. Similar results for a different templates are shown in Table 1.

Contaminations	ARC-Easy (1172 quest.)		ARC-Challenge (2373 quest.)		MMLU* (5000 quest.)	
	$\log_{10}(p)$	Acc. (% Δ)	$\log_{10}(p)$	Acc. (% Δ)	$\log_{10}(p)$	Acc. (% Δ)
0	-0.3	51.7 (+0.0)	-0.3	28.5 (+0.0)	-0.9	30.4 (+0.0)
4	-3.0	61.3 (+9.9)	-1.2	35.1 (+7.0)	-5.7	36.9 (+6.5)
8	-5.5	68.2 (+16.9)	-4.5	42.2 (+14.1)	<-12	43.0 (+12.6)
16	<-12	84.1 (+32.8)	<-12	65.3 (+37.2)	<-12	62.1 (+31.7)

B PROOF OF CORRECTNESS FOR CONTAMINATION DETECTION

We give the proof of Proposition 1. We remind that \mathcal{H}_0 is “The cumulative score S follows a binomial distribution $B(\tilde{N}, 0.5)$ ” and $p\text{-value}(s) = \mathbb{P}(S(X_N) \geq s \mid \mathcal{H}_0) = I_\gamma(s+1, N-s)$ and:

Proposition 1. *If we define “being contaminated” as having memorized the watermark, then “not being contaminated” matches $\mathcal{H}_0 := S \sim B(\tilde{N}, 1/2)$. Therefore, the test T_α (that rejects \mathcal{H}_0 if the p-value is less than α) correctly tests for contamination, and has a False Positive Rate equal to α .*

Proof. Assume that “ M has not memorized watermark bias with secret key s ”. Since the summed scores are i.i.d. due to de-duplication, and independent of the watermarking process because the suspect model has no other knowledge about s , and because we exclude the possibility of simply repeating watermarked tuples from the prompt through de-duplication, there is no bias towards the green or red

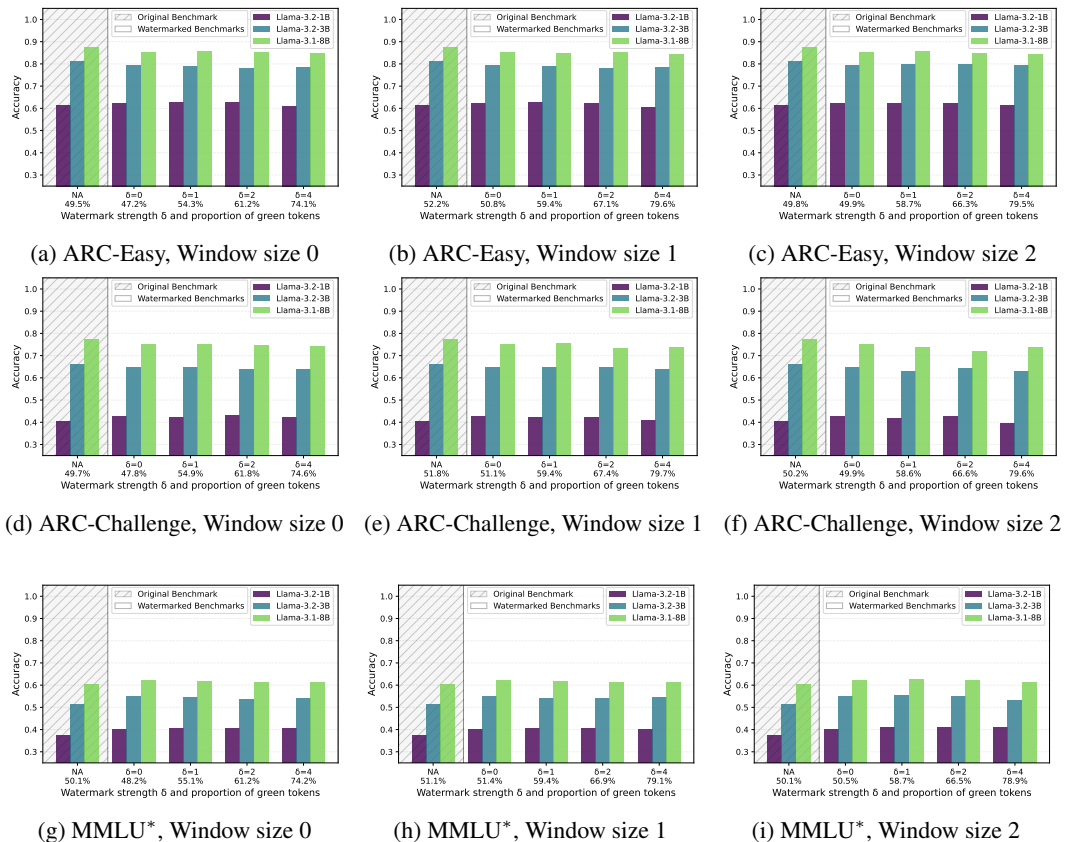


Figure 7: Comparison of Llama3 model performance on various versions of ARC-Easy, ARC-Challenge, and MMLU* for different watermark window sizes. Each row corresponds to a different dataset, and each column corresponds to a different window size. The window size does not noticeably impact the benchmark’s utility.

tokens specific to s . Therefore, the indicators $\mathbb{1}(y^{(t)} \text{ is in the greenlist of } (s, (x^{(t-i+1)})_{i=k}^1))$ are i.i.d. simulations distributed according to a Bernoulli distribution with parameter 0.5 (in expectation over the keys). Thus, S follows a binomial distribution $B(\tilde{N}, 0.5)$. So, \mathcal{H}_0 is true.

Reciprocally, if \mathcal{H}_0 is True, then there is no bias towards the green tokens, which by definition means that it has not memorized the watermark. The p -value is exactly the probability to observe a score as extreme as s under H_0 , so it is the probability to observe a score as extreme as s if M has not memorized the watermark with secret key s present in the benchmark. Now let T_α be the test that rejects \mathcal{H}_0 if the p -value is less than α . It correctly tests for contamination, and has a FPR of α . \square

C COMPUTE RESOURCES

We use our internal cluster with A-100 GPUs with 80GB memory, and:

- Each radioactivity detection test took less than 30 minutes on a single GPU. We processed the benchmark through the model, which contains a maximum of 325k tokens for MMLU* (see 1).
- Pretraining of the 1B models was conducted on 8 nodes (so 64 GPUs) and took approximately six hours. Training of smaller models, with 360M and 135M parameters, was performed on 4 nodes, taking 2 hours and 1 hours respectively.

Overall, we estimate that training the 1B models required approximately 5,000 GPU hours, calculated as 3 (different window sizes) x 4 (different degrees of contamination) x 6 x 8 x 8 (GPU hours for training). We approximate an additional factor of 2 for the other models trained, resulting in a total of approximately 10,000 GPU hours.

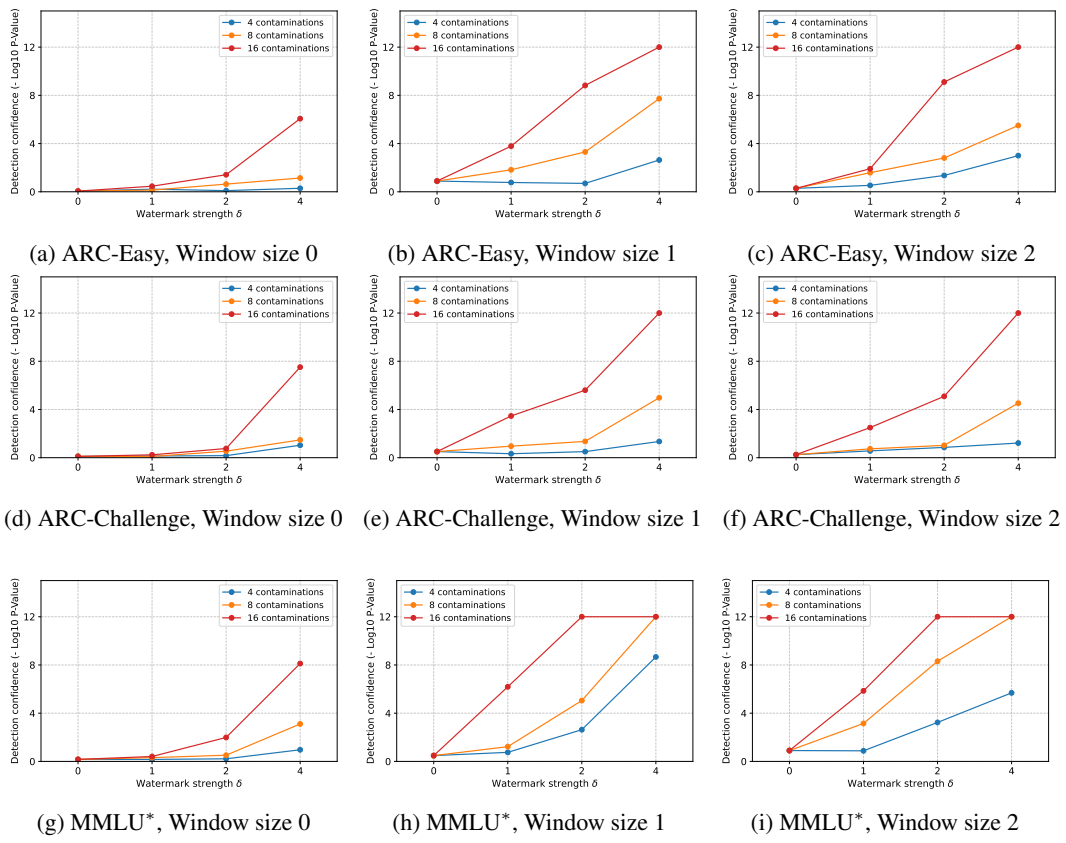
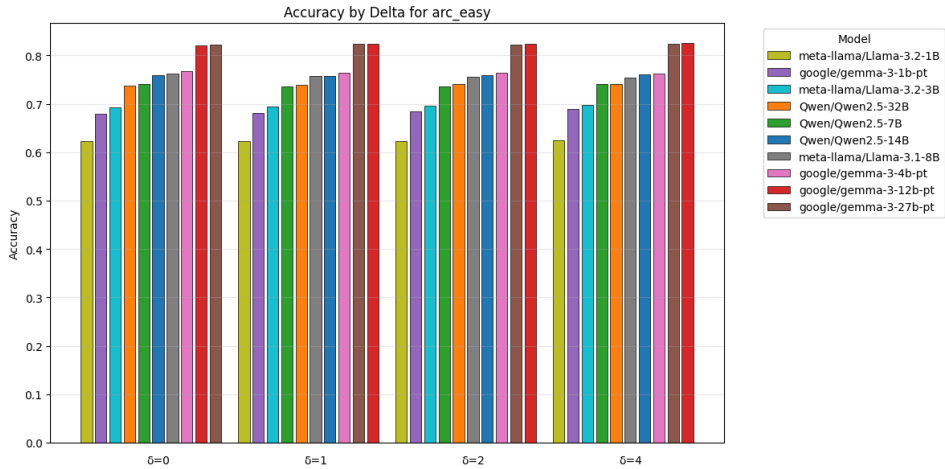


Figure 8: Comparison of radioactivity detection on various versions of ARC-Easy, ARC-Challenge, and MMLU* for different watermark window sizes. Each row corresponds to a different dataset, and each column corresponds to a different window size. Bigger benchmarks leads to easier detection, and window size impacts the detection confidence, the larger the better, accross all benchmarks.

918 D ADDITIONAL RELATED WORK AND EXPERIMENTS AFTER REBUTTAL
919
920
921

922 **Quality assessment of watermarked benchmarks.** Following the rebuttal, we evaluate other
923 families of models on the watermarked benchmark. Specifically, we evaluate Qwen (Bai et al., 2023)
924 and Gemma-3 (Team et al., 2025) models on the benchmarks. Figure 9 shows that for different
925 watermark strength, the performance of the models is still maintained.



922 Figure 9: Performance of Llama-3 (Grattafiori et al., 2024), Qwen (Bai et al., 2023) and Gemma-3 (Team et al.,
923 2025) models on different rephrased versions of Arc-easy. Performance is maintained.